Single sensor for multiple analytes employing fluorometric differentiation for Cr^{3+} and Al^{3+} in semi-aqueous medium with bio-activity and theoretical aspects

Malay Dolai[a,*], Urmila Saha[b], Avijit Kumar Das[c,d,*] and Gopinatha Suresh Kumar[b]

Table S1. Crystal data and structure refinement for H$_2$SALNN.

Parameters	(CCDC No.1814623)
Formula	C$_{16}$ H$_{16}$ N$_2$ O$_4$
Formula Weight	300.31
Crystal System	Monoclinic
Space group	P21/n (No. 14)
a, b, c [Å]	10.3695(13) 6.0922(8) 11.4055(15)
α, β, γ [^{o}]	90 98.355(2) 90
V [Å^3]	712.87(16)
Z	2
D(calc) [g/cm^3]	1.399
μ(MoK$_\alpha$) [/mm]	0.102
F(000)	316
Crystal Size [mm]	0.24 x 0.28 x 0.55
Temperature (K)	100
Radiation [λ, Å]	0.71073
Theta Min-Max [^{o}]	2.5, 31.4
Dataset	-15: 15 ; -8: 8 ; -16: 16
Tot., Uniq.Data, R(int)	3328, 2013, 0.013
Observed data [I > 2σ(I)]	1834
N$_{ref}$, N$_{par}$	2013, 105
R, wR_2, S	0.0405, 0.1172, 1.05
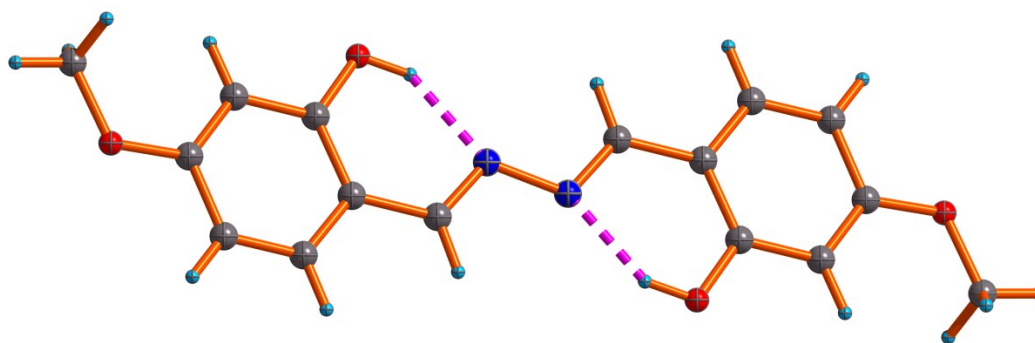
Fig.S1: The ORTEP view of centro-symmetric H$_2$SALNN ligand.
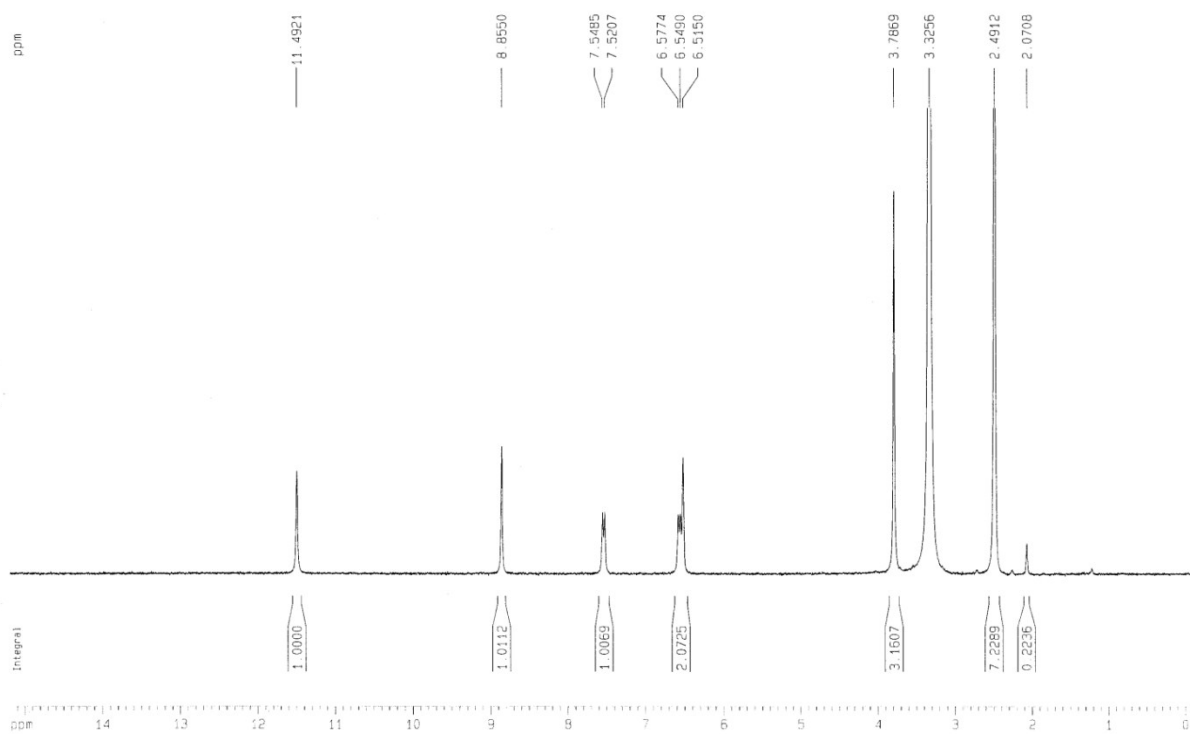
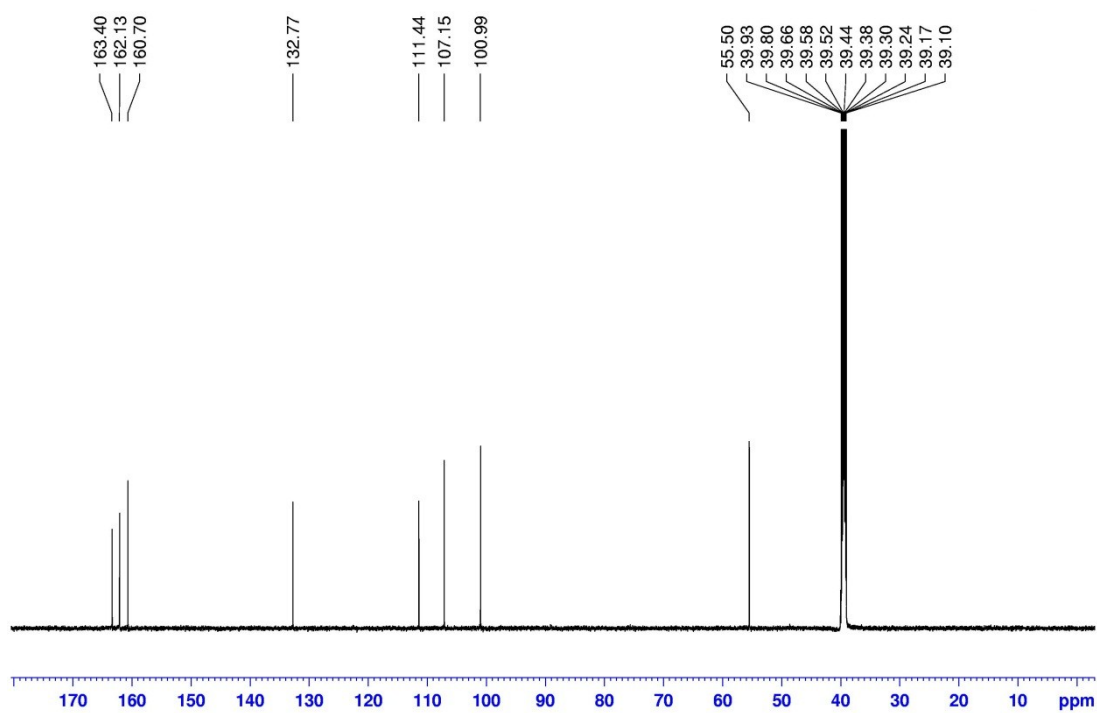**Fig.S2**: ^{1}H-NMR spectra of ligand- H_2SALNN

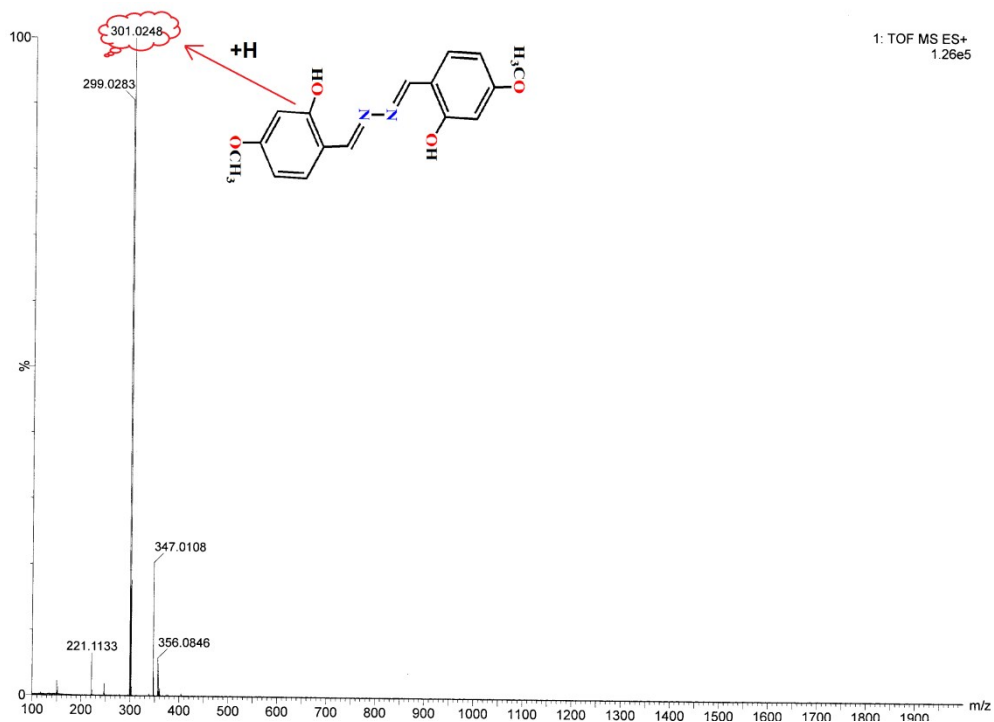**Fig.S3**: ^{13}C-NMR spectra of ligand- H_2SALNN

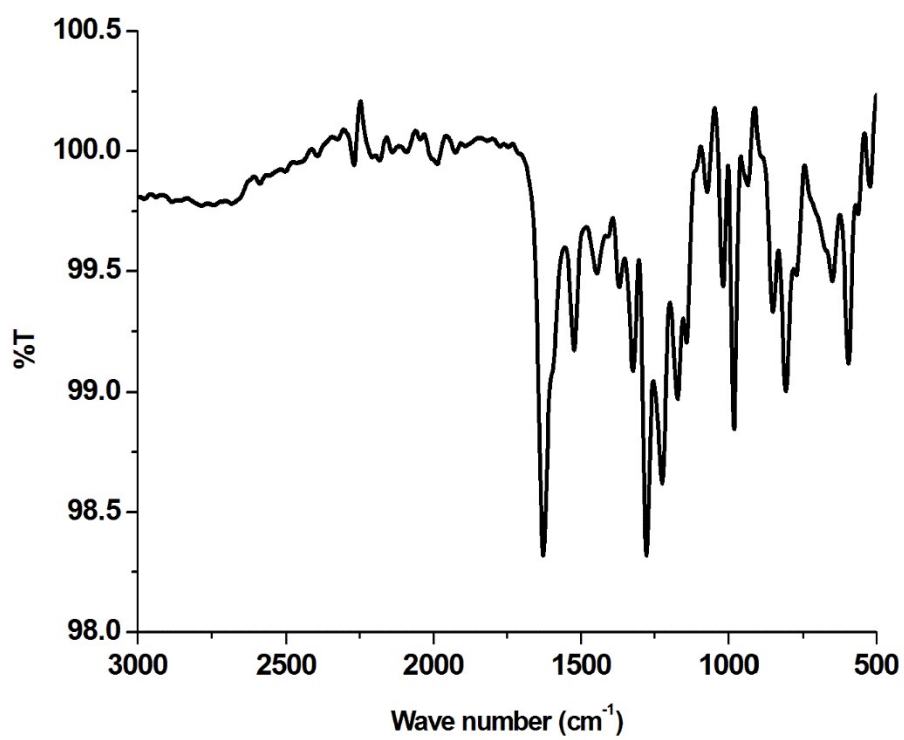**Fig.S4**: ESI-MS spectra of ligand- H$_2$SALNN
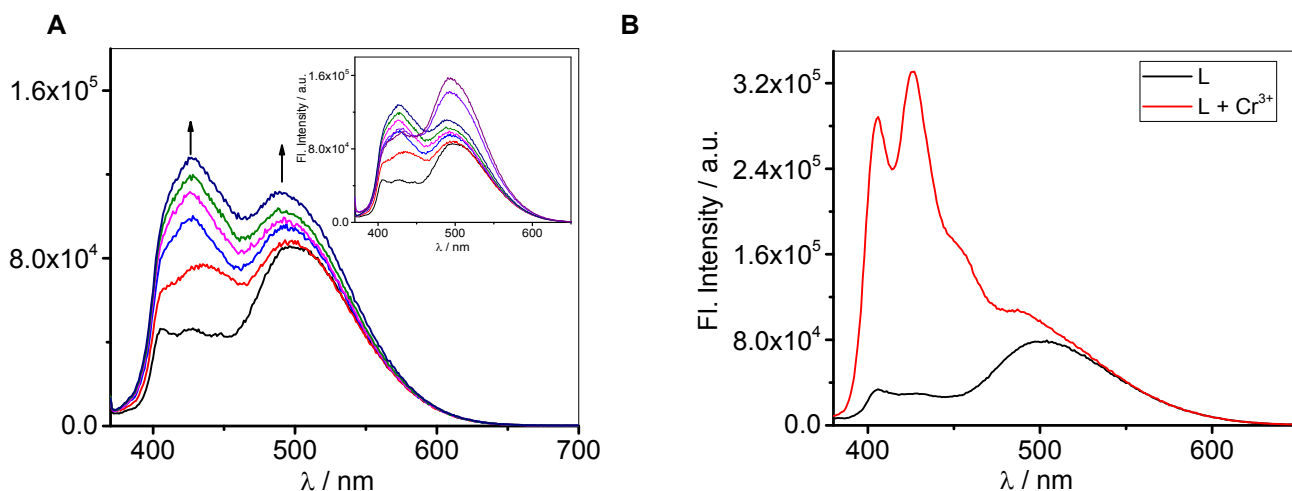

Fig.S5: Infra-red(IR) spectra of ligand- H$_2$SALNN.

Figure S6A. The trend of increase of emission intensity at the receptor H2SALNN (c = 2x10^{-5} M) with Al^{3+} (c = 2x10^{-4} M) at low concentration of Al^{3+}. Inset: The change of emission intensity at high con. of Al^{3+} ion. **B**. The initial trend for the change of emission intensity at the receptor H2SALNN (c = 2x10^{-5} M) with Cr^{3+} (c = 2x10^{-4}).
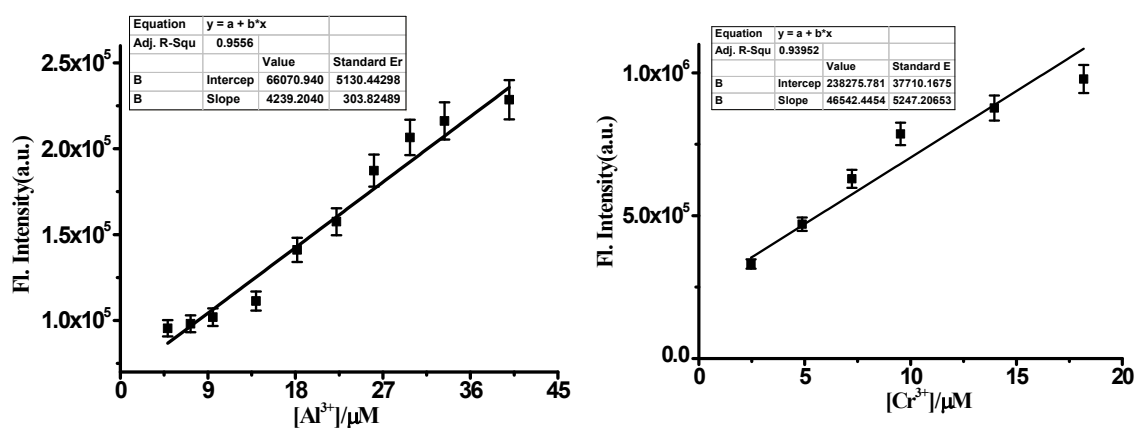
Calculation of detection limit:

Fig. S7: (a) Changes of emission intensity of **H₂SALNN** (c = 2 x10^{-5}M) as a function of [Al^{3+}] (c = 2x10^{-4}M) at 490 nm. **(b)** Changes of emission intensity of **H₂SALNN** (c = 2 x10^{-5}M) as a function of [Cr^{3+}] (c = 2x10^{-4}M) at 427 nm.

The detection limit (DL) of **H₂SALNN** towards Al^{3+} and Cr^{3+} in emission spectra was determined from the following equation:

DL = K* Sb$_l$/S

Where K = 2 or 3 (we take 2 in this case); Sb$_l$ is the standard deviation of the blank solution; S is the slope of the calibration curve.

From the graph Fig.S9(a), we get slope = 4239.20, and Sb_1 value is 9430.42.

Thus using the formula we have detected the fluorescence of **H₂SALNN** using mininum 4.3 μM of Al^{3+} solution.

From the graph Fig.S9(b), we get slope = 46542.44, and Sb1 value is 71412.33.

Thus using the formula we have detected the fluorescence of **H₂SALNN** using mininum 3.40 μM Cr^{3+}.

Determination of fluorescence quantum yield:

Here, the quantum yield φ was measured by using the following equation,

$\varphi_x = \varphi_s (F_x / F_s)(A_s / A_x)(n_x^2 / n_s^2)$

Where,

X & S indicate the unknown and standard solution respectively, φ = quantum yield,

F = area under the emission curve, A = absorbance at the excitation wave length,

n = index of refraction of the solvent. Here φ measurements were performed using anthracene in ethanol as standard [φ = 0.27] (error ~ 10%)

Association constant determination:

The binding constant value of metal ions Al^{3+} and Cr^{3+} with the **H₂SALNN** has been determined from the emission intensity data following the modified Benesi–Hildebrand equation, $1/\Delta I = 1/\Delta I$ max + $(1/K[C])(1/\Delta I$ max$)$. Here ΔI = I-Imin and ΔI max = Imax-Imin, where Imin, I, and Imax are the emission intensities of sensor considered in the absence of guest , at an intermediate concentration and at a concentration of complete saturation of guest where K is the binding constant and [C] is the guest concentration respectively. From the plot of (Imax-Imin)/(I-Imin) against $[C]^{-1}$ for sensor, the value of K has been determined from the slope. The association constant (K_a) as determined by fluorescence titration method for **H₂SALNN** with Al^{3+} is found to be 1.4 x $10^4 M^{-1}$ (error < 10%) and Cr^{3+} towards **H₂SALNN** is 1x$10^5 M^{-1}$.

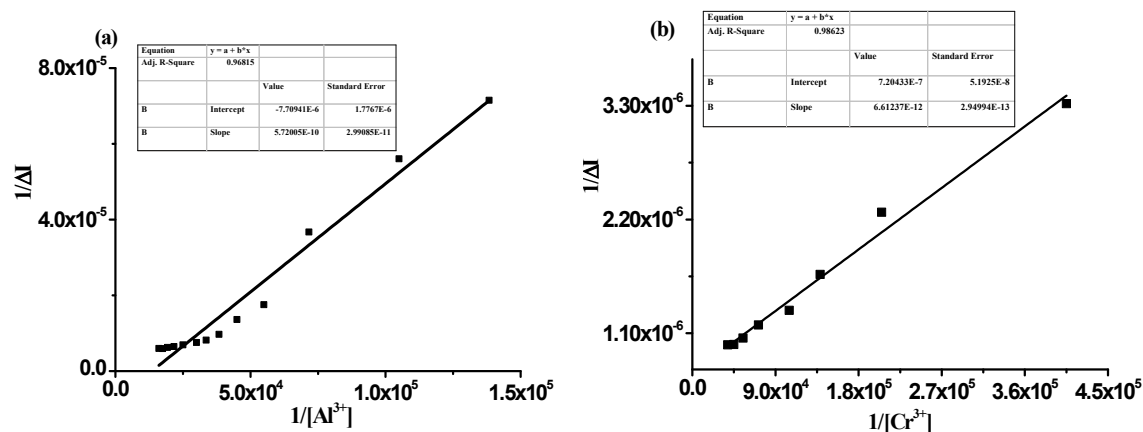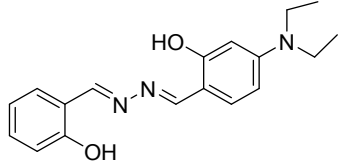**Fig. S8:** (a) Benesi–Hildebrand plot from fluorescence titration data of H₂SALNN (20μM) with Al³⁺. (b) Benesi–Hildebrand plot from fluorescence titration data of H₂SALNN (20μM) with Cr³⁺.
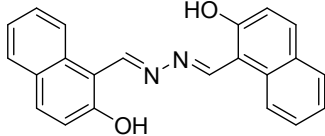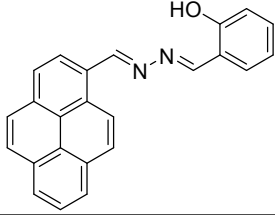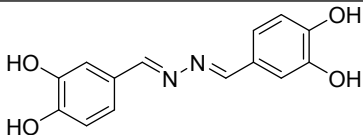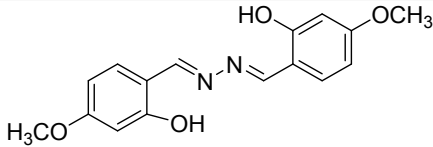
Table S2: The comparison of H₂SALNN with other hydrazine ligands with the substitution on the basis of different metal ion binding.

Entry	Ligand structures	Binding metal ions	References
1.		Ti	(a)
2.		Fe^{3+} Cu^{2+}, Al^{3+}	(b) (c)
3.		Zn^{2+}	(d)
4.		Zn^{2+} Cu^{2+}	(e) (f)

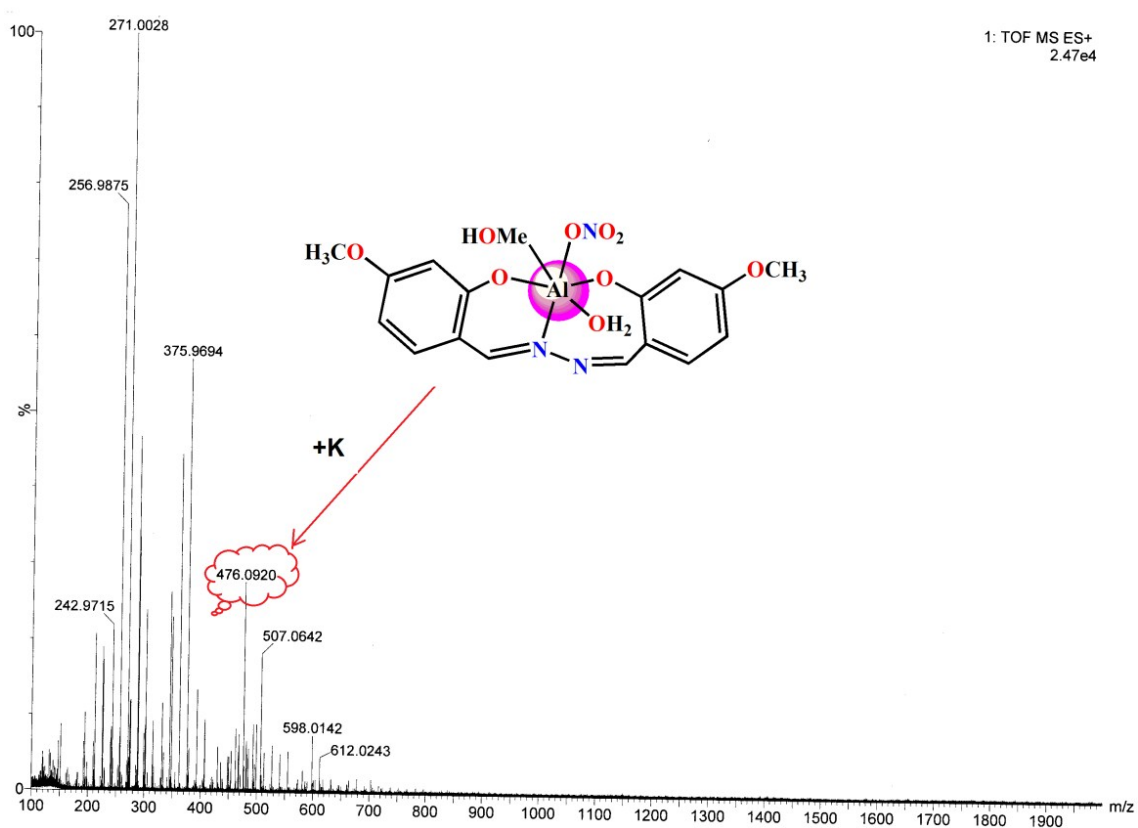| 5.		Cu^{2+}	(g)
6		Cu^{2+} Al^{3+}	(h) (i)
7		Zn^{2+}	(j)
8		Co^{3+}	(k)
9		Al^{3+} and Cr^{3+}	This work

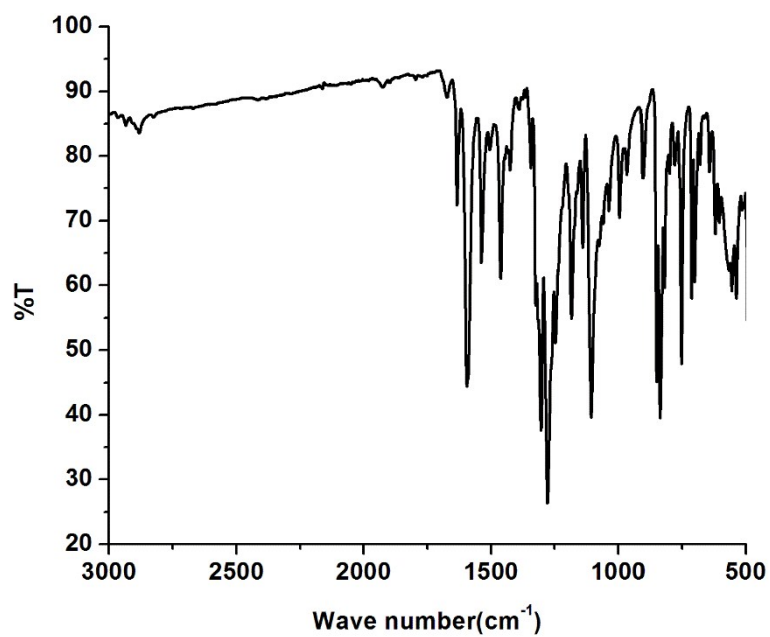**Fig.S9**: ESI-MS spectra of complex-1

Fig.S10: Infra-red(IR) spectra of complex-1
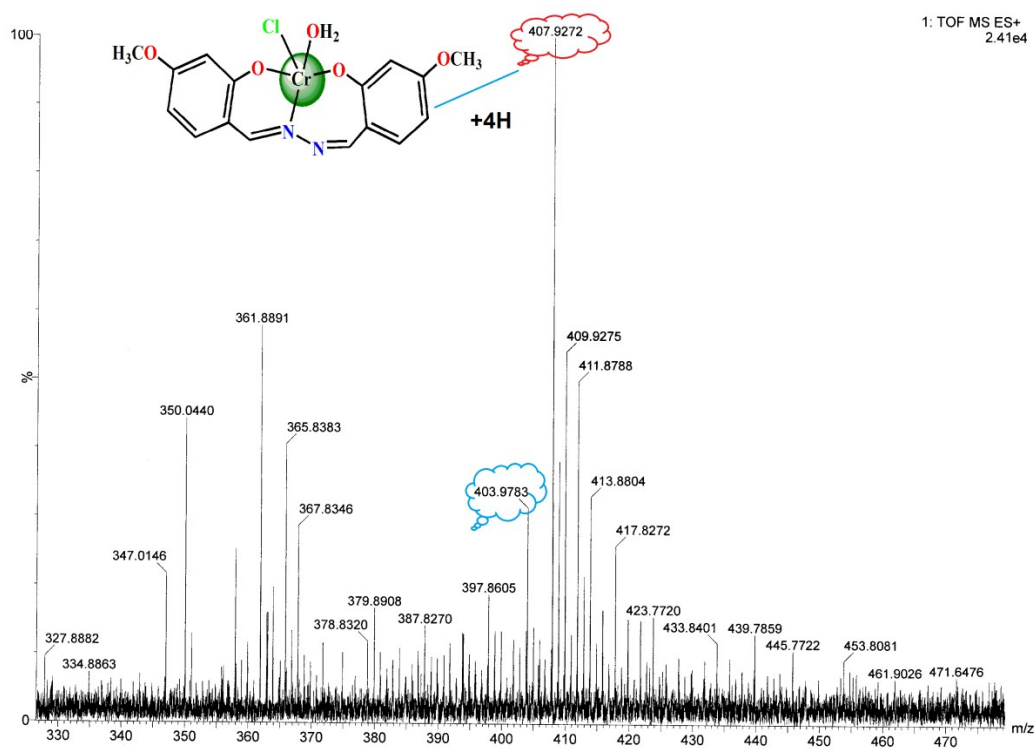

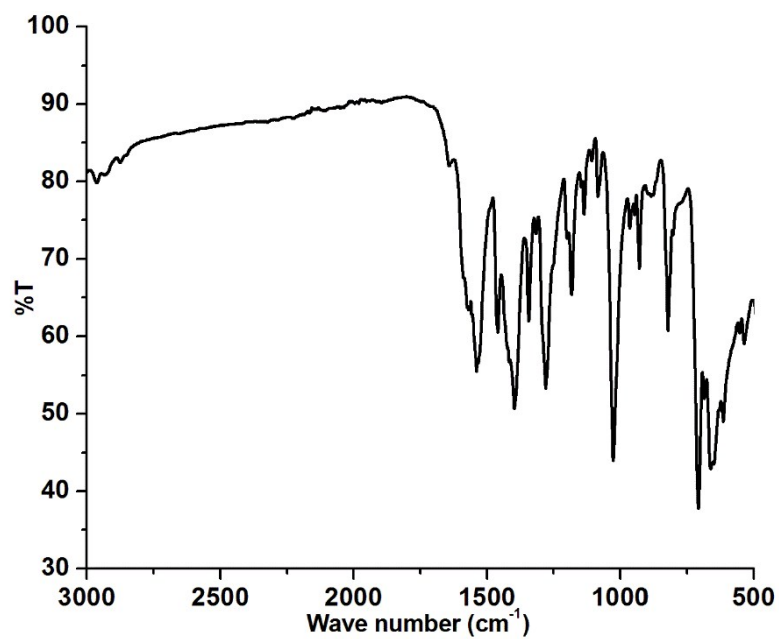**Fig.S11**: ESI-MS spectra of complex-2
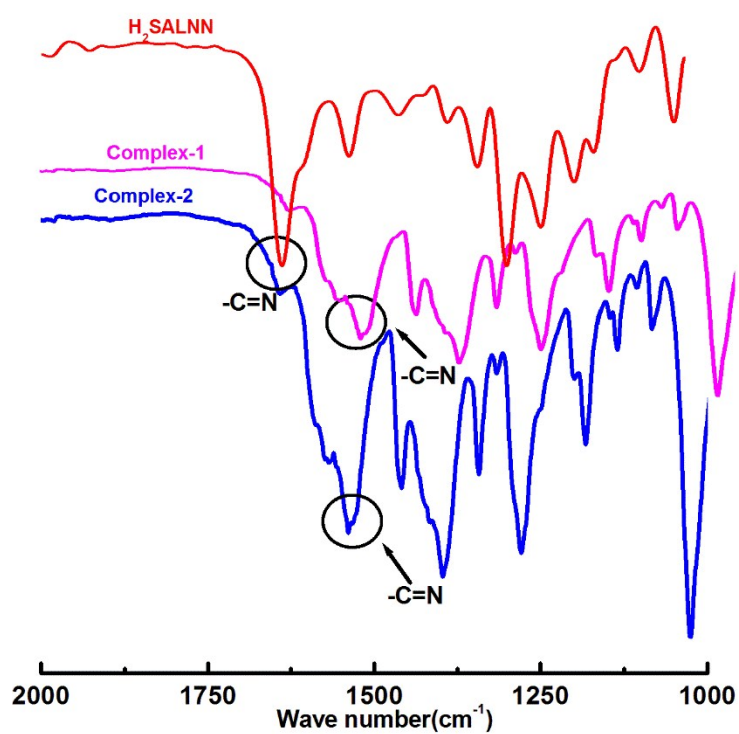
Fig.S12: Infra-red(IR) spectra of complex-2

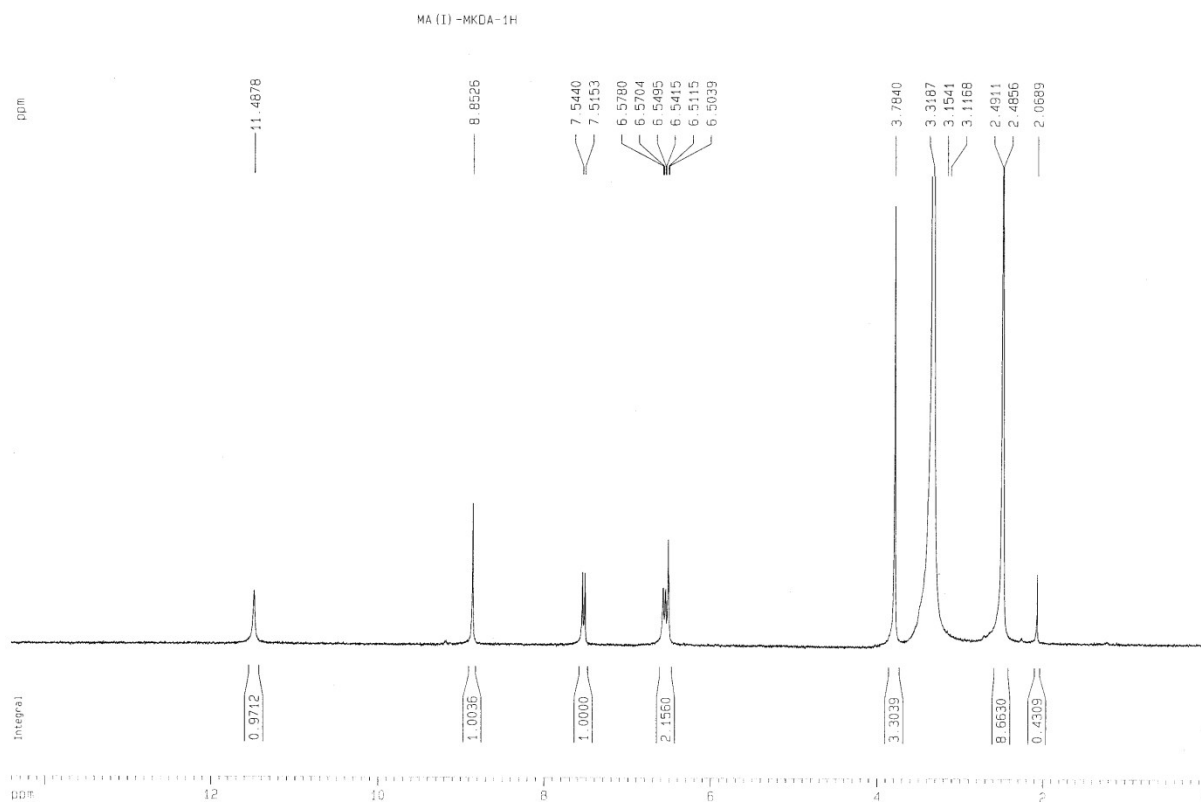**Fig.S13**: Compared infra-red(IR) spectra of H₂SALNN, complex-1 and complex-2.

Fig.S14: ^{1}H-NMR spectra of 0.5 equivalent addition of Al^{3+} on H_2SALNN.
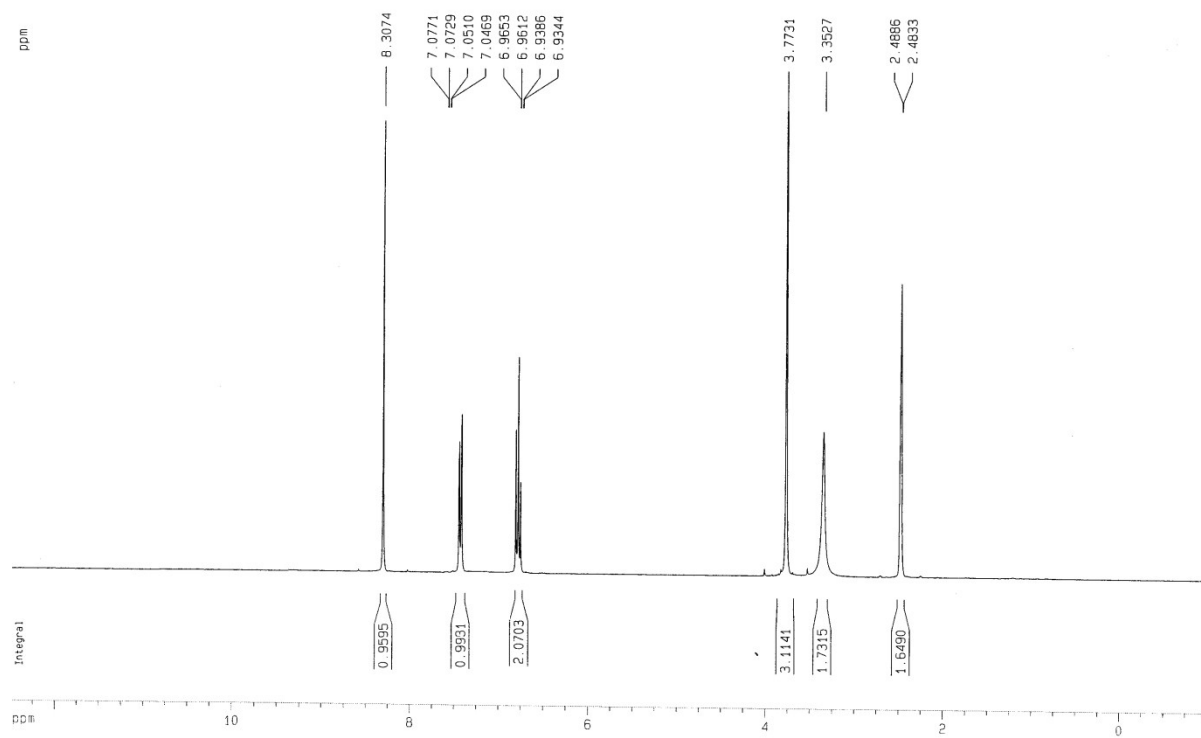

Fig.S15: ^{1}H-NMR spectra of 1 equivalent addition of Al^{3+} on H_2SALNN.

Table S3. Hydrogen bonds for H$_2$SALNN [Å and °].

D-H...A	d(D-H)	d(H...A)	d(D...A)	<(DHA)
C(8)-H(8A)...O(2)#2	0.98	2.49	3.2540(12)	134.4
C(8)-H(8C)...O(1)#3	0.98	2.59	3.3488(12)	134.0
O(1)-H(1)...N(1)	0.883(17)	1.855(17)	2.6475(10)	148.3(16)

Symmetry transformations used to generate equivalent atoms:

#1 -x,-y+1,-z+1   #2 -x+3/2, y-1/2,-z+1/2   #3 -x+1,-y,-z+1

References:

(a) H. C. Tseng, H. Y. Chen, Y. T. Huang, W. Y. Lu, Y. L. Chang, M. Y. Chiang, Y. C. Lai, and H. Y. Chen, *Inorg. Chem*., 2016, **55**, 1642–1650.

(b) M. Hong, G. Dong, D. Chun-ying, L. Yu-ting and M. Qing-jin, *J. Chem. Soc., Dalton Trans*., 2002, 3422–3424.

(c) C. Gou, S. H. Qin, H. Q. Wu, Y. Wang, J. Luo, X. Y. Liu, *Inorganic Chemistry Communications* 2011, **14,** 1622–1625.

 (d) M. G. Mohamed, R. C. Lin, J. H. Tu, F. H. Lu, J. L. Hong, K. U. Jeong, C. F. Wangd and S. W. Kuo, *RSC Adv*., 2015, **5**, 65635–65645.

(e) D. X. Xie, Z. J. Ran, Z. Jin, X. B. Zhang, D. L. An, *Dyes and Pigments* 2013, **96**, 495-499.

(f) J. Huo, K. Liu, X. Zhao, X. Zhang , Y. Wang, Spectrochimica Acta Part A: Molecular and Biomolecular Spectroscopy 2014, **117**, 789–792.

(g) K. Tiwari, S. Kumar, V. Kumar, J. Kaur, S. Arora, R. K. Mahajan, Spectrochimica Acta Part A: Molecular and Biomolecular Spectroscopy 2018, **191**, 16–26.

(h) T. Sun, Q. Niu, T. Li, Z. Guo, H. Liu, Spectrochimica Acta, Part A: Molecular and Biomolecular Spectroscopy 2018, **188**, 411-417.

(i) A. Ghosh, A. Sengupta, A. Chattopadhyay and D. Das, RSC Adv., 2015, **5**, 24194-24199

(j) Z. Kowser, U. Rayhan, S. Rahman, P. E. Georghiou, T. Yamato, *Tetrahedron* 2017, 73, 5418-5424.

(k) Y. Suenaga, and C. G. Pierpont, Inorganic Chemistry, Vol. 44, No. 18, 2005.